Toxicology in Vitro 58 (2019) 42–50

Contents lists available at ScienceDirect

Toxicology in Vitro

journal homepage: www.elsevier.com/locate/toxinvit

VIVD: Virtual *in vitro* distribution model for the mechanistic prediction of intracellular concentrations of chemicals in *in vitro* toxicity assays

Fisher C.[a,*], Siméon S.[b], Jamei M.[a], Gardner I.[a], Bois Y.F.[b]

[a] Certara UK Limited, Simcyp Division, Acero, 1 Concourse Way, Sheffield S1 2BJ, UK
[b] INERIS, METO Unit, Verneuil en Halatte, France

ARTICLE INFO

Keywords:
In vitro assays
IVIVE
Biokinetics
Toxicity

ABSTRACT

In vitro toxicity testing routinely uses nominal treatment concentrations as the driver for measured toxicity endpoints. However, test compounds can bind to the plastic of culture vessels or interact with culture media components, such as lipids and albumin. Additionally, volatile compounds may partition into the air above culture media. These processes reduce the free concentrations of compound to which cells are exposed.

Models predicting the freely dissolved concentrations by accounting for these interactions have been published. However, these have only been applied to neutral compounds or assume no differential ionisation of test compounds between the media and cell cytoplasm. Herein, we describe an *in vitro* distribution model, based on the Fick-Nernst Planck equation accounting for differential compound ionisation in culture medium and intracellular water. The model considers permeability of ionised and unionised species and accounts for membrane potential in the partitioning of ionised moieties. By accounting for lipid and protein binding in culture medium, binding to cell culture plastic, air-partitioning, and lipid binding in the cell, the model can predict chemical concentrations (free and total) in medium and cells. The model can improve *in vitro in vivo* extrapolation of toxicity endpoint by determining intracellular concentrations for translation to *in vivo*.

1. Introduction

Integrated testing strategies (ITSs), combining *in vitro* assay systems, *in silico* methodologies, knowledge-bases, and omics driven mechanistic insights are increasingly replacing the use of animal models in toxicological risk assessment. This has been driven, not only by the increasing availability and applicability of these technologies, but also by an increasing societal and legislative impetus to refine, reduce and, ultimately, replace animal testing. The 3Rs principle, applied to the use of animal models, is not solely based on ethical considerations of animal welfare, but also on the increasing acceptance that extrapolation from preclinical species to humans is not sufficiently robust for risk

Abbreviations: Φ, membrane potential (mV); ΔU_{aw}, internal energy of phase change for air to water partitioning; ΔU_{ow}, internal energy of phase change for octanol to water partitioning; *[AP-]*, concentration of acidic phospholipids; C_{air}, concentration in the air in the headspace; C_{cell}, total intracellular concentration; $C_{medium,dissolved,u}$, unbound, dissolved medium concentration; $C_{nominal}$, nominal test concentration in medium; $C_{plastic}$, concentration bound to plastic; $Cell_{diam.}$, diameter of a single cell; CoA, certificate of Analysis; *F*, Faraday constant; FBS, fetal Bovine Serum; f_{iw}, fractional cellular volume of intracellular water; f_{lyso}, fractional cellular volume of lysosome; f_{mito}, fractional cellular volume of mitochondria; f_{nl}, fractional cellular volume of neutral lipid; f_{np}, fractional cellular volume of neutral phospholipids; $f_{protein}$, fraction of FBS comprising albumin; $f_{nl,FBS}$, fraction of FBS comprised of neutral lipid; $f_{protein}$, fraction of FBS comprising albumin; f_{serum}, fraction of culture medium comprised of FBS; fu_{FBS}, fraction unbound in FBS; $fu_{FBS,dilu}$, fu_{FBS} corrected for dilution in complete culture medium; f_{ui}, fraction unionised; ITS, integrated testing strategy; IVIVE, *in vitro in vivo* extrapolation; *K*, Kelvin; *KaAP*, acidic phospholipid association constant; $k_{air,u}$, air to water partition coefficient; $k_{cell,u}$, ratio of total cell concentration to unbound medium concentration; $k_{cell,uuuu}$, ratio of the unbound, unionised concentration in the cell and the culture medium; k_H, Henry's law constant; $K_{IW,uuuu}$, ratio of the unbound, unionised concentration in the intracellular water cell and the specified organelle; $k_{plastic,u}$, plastic to culture medium partition coefficient; $k_{protein}$, albumin to water partition coefficient; PAH, polycyclic aromatic hydrocarbons; P_i, partial pressure of the gas phase of the compound; P_{nl}, neutral lipid partition coefficient; P_{np}, neutral phospholipid partition coefficient; P_{ow}, octanol-water partition coefficient; *PSV*, partial specific volume; $P_{vo:w}$, olive oil-water partition coefficient; *R*, universal gas constant; $SA_{medium\ plastic}$, surface area of plastic culture vessel in contact with culture medium (m^2); $System_{diam.}$, diameter of culture system (mm); TAG, triacylglyceride; T_{ref}, reference temperature parameters are experimentally determined or predicted; T_{sys}, temperature of the cell culture system; V_{air}, volume of air in head space above culture medium (L); V_{medium}, volume of culture medium (µL); $V_{total\ cell}$, total volume of cultured cells (L); V_{well}, volume of a culture vessel (µL); *Y*, concentration ratio of ionised to unionised ionisable compound

* Corresponding author.
E-mail address: ciaran.fisher@certara.com (C. Fisher).

https://doi.org/10.1016/j.tiv.2018.12.017
Received 27 September 2018; Received in revised form 21 December 2018; Accepted 27 December 2018
Available online 29 December 2018

assessment in the 21st century (Gibb, 2008; Holmes et al., 2010).

Cell based *in vitro* systems can be used to determine the concentration dependant response for a range of toxicological endpoints, from simple cytotoxicity assays, to highly tissue-specific functional or transcriptomic responses (Godoy et al., 2013; Meek and Lipscomb, 2015). The use of such assays seeks to inform a more mechanistic understanding of the pathways that mediate adverse outcomes (Leist et al., 2017). *In vitro* assays are ideally placed to operate in this way since target-organ, species-specific material can be used in these model systems, and they are amenable to scaling to high-throughput screening approaches. The Tox21 project seeks to utilise *in vitro* assays in such an approach in order to assess the hazard for a huge number of compounds for which *in vivo* data is unavailable and realistically unobtainable (Tice et al., 2013). Based on the data generated, an *in vitro in vivo* extrapolation (IVIVE) approach can then be adopted in assessing human and animal hazard (Bell et al., 2018).

However, toxicological endpoints quantified *in vitro* are routinely correlated to a range of nominal treatment concentrations to establish a dose-response relationship. Yet, using the nominal treatment concentration as the driving concentration for toxicity is inaccurate since it does not account for the differential distribution of compounds within the test system that will determine the true free concentration available for distribution into the cell, and subcellular compartments, and so determine the driving concentration for toxicity at the target site. In order to have a more accurate assessment of concentration driven toxicity, it is necessary to correct the nominal treatment concentration, accounting for the different factors affecting a compounds distribution. These include binding to the plastics used in cell culture, exchange at the interface between culture medium and the air in the headspace, and binding to components within serum that may be included in culture medium (*e.g.* lipids and proteins); the modelling of these processes is termed biokinetics (Blaauboer, 2010).

A number of steady-state biokinetic models have been published that account for some or all of the factors listed above. Armitage and colleagues (Armitage et al., 2014) published a model framework to predict intracellular concentrations, correcting for some of the distribution factors in monolayer cell culture. This steady-state framework assumes instantaneous partitioning between media, headspace, serum-lipids, serum-proteins, dissolved organic material, and the cultured cell volume. The steady-state assumption lends itself to the modelling of non-proliferating cells, at the time of the assay, with minimal metabolic activity against the test compound. Moreover, a critical assumption of the Armitage model is that the test compounds are neutral or not significantly ionised under the conditions of the *in vitro* assay. This assumption of neutrality was, to some degree, addressed in the model developed by Fischer *et al* (Fischer et al., 2017) where the authors adopted the same steady-state assumption, but excluded the partitioning of compound into the headspace. The authors incorporated separate partition constants for both the ionised and unionised fraction of test compound, determining the fraction ionised assuming a uniform pH = 7.4 throughout the test system. This neglects the differential ionisation potential between the culture media and intracellular water resulting from their differing pH. Furthermore, the interior of the cell itself is not a uniform environment with the interior of specific organelles being maintained at a specific pH critical to their function (*i.e.* lysosomes (pH ≈ 4.5), mitochondria (pH ≈ 8), cytosol (pH ≈ 7). Indeed, the differential ionisation of compounds between organelles and intracellular water can result in the preferential sequestration of compounds within organelles; a phenomena commonly known by the misnomer 'ion-trapping' (Kazmi et al., 2013). It is also critical to note that differences in the intrinsic permeability of the unionised/ionised form are not the only factors determining the distribution of ionised compound into cells. The potential difference maintained across the cell membrane, membrane potential (Φ, mV), can actively promote the uptake or exclusion of ionised compounds from the cell interior and can vary significantly between cell types. It is important to remember that these models (Armitage et al., 2014; Fischer et al., 2017) are steady-state approximations of multiple dynamic processes. Critically, they assume that the loss of test compounds within the *in vitro* system is negligible with no loss through metabolic clearance or instability. When that is not the case, the steady-state assumption may lead to overestimation of intracellular concentrations of the parent molecule, particularly for highly metabolized chemicals. Obviously, this restricts the applicability of these models and limits their use in the assessment of ionisable or metabolically cleared compounds. Dynamic (ODE-based) models that move beyond the steady-state assumptions described have been published incorporating metabolic clearance and distribution into mitochondria (Worth et al., 2017; Zaldivar Comenges et al., 2017). However, these models still assume no significant ionisation of the test compound.

Here we propose two versions of an improved virtual *in vitro* intracellular distribution (VIVD) model: the first is a steady-state formulation which relates a molecule's distribution to its ionisation state, membrane permeability, and volatility. The VIVD model also accounts for cell membrane potential, pH, and extracellular binding to culture medium proteins, lipids, and plastics, but metabolism is considered negligible. The second is a quasi-steady-state dynamic formulation incorporating metabolic clearance which can be used when metabolic loss of compound cannot be considered negligible. The impact of the various improvements proposed are illustrated through simulations.

2. Materials and methods

The model structure described below assumes monolayer cell culture in wells (*i.e.* plate format) or in round dishes; this distinction is only important in considering test compound binding to plastic cultureware and will be discussed below. The parameterization used herein assumes a monolayer culture of primary human hepatocytes. But the model can easily be adapted to predict distribution into other cell types by including cell specific system parameters (see below for further explanation).

The (*in vitro)* systems parameters for the model described herein, which are independent of the test compounds, can be subdivided into two categories; those related to cultured cells and those pertaining to the culture conditions. Each of these will be described below. Default units for calculations within the model are litres (*L*) for volume, metres (m) for length/area and molar for concentration (M).

2.1. Cell composition

Hepatocytes account for ~60% of the cells in the liver and account for 80% of the parenchymal volume (Godoy et al., 2013). Here, we assume that viable isolated human hepatocytes will maintain a comparable size and composition with respect to lipids as to hepatocytes within human liver. The diameter of human hepatocytes has been cited as being between 20 and 40 μm, while mouse hepatocytes have been reported as being 23.3 ± 3.1 μm in diameter (Hoehme et al., 2010; Schwen et al., 2015). Here we take 30 μm to be the diameter of human hepatocytes in 2D culture, $Cell_{diam.}$ (μm). Assuming that cells cultured in a 2D-monolayers take a dome-like shape (half-spheres) on the culture surface, and knowing the number of cells at the time of the assay, we can calculate the total volume of cells, $V_{total\ cell}$, using Eq. (1).

$$V_{total\ cell}(L) = n_{cell}\left(\frac{\frac{4}{3}\pi(Cell_{diam.}\bullet 0.5e^{-6})^3}{2}\right)\bullet 10^3 \quad (1)$$

2.2. Culture conditions

The formats available for cell culture are diverse. However, the adoption of high-throughput and automated methods has necessitated a degree of standardisation across these formats. In most cases high-

throughput assays are conducted in plate formats comprising cylindrical wells. The model assumes a hermetically sealed, cylindrical culture system corresponding to an individual well of a culture plate or a single culture dish. Based on this assumption, the model can be easily parameterised to reflect the diverse range of culture plate formats that are commercially available. Four culture condition parameters are required to define the system that is being used: diameter of a single culture vessel ($System_{diam.}$; mm), volume of the culture system (V_{well}; µL), the volume of medium (V_{medium}; µL) and the fraction of medium (*v*/v) comprising fetal bovine serum (FBS) (f_{serum}). More specialised culture mediums, where serum is pretreated (*e.g.* delipidized), or serum free systems where specific concentrations of lipid or albumin are added can also be simulated.

The volume of air (V_{air}; *L*), above the medium can be calculated using Eq. (2) and is subsequently used to calculate the concentration of test compound partitioned into the headspace at steady state.

$$V_{air} = 10^{-6}(V_{well} - V_{medium}) - V_{totalcell} \quad (2)$$

To calculate the binding of test compound to plastic it is necessary to calculate the surface area of plastic in direct contact with the medium, $SA_{medium\ plastic}$ (m^2), Eq. (3). Here we assume a round well culture system and so the only variables will be the diameter of the well and the volume of medium.

$$SA_{medium\ plastic} = 2\pi r\left(\frac{V_{medium} \bullet 10^{-9}}{\pi\,(system_{diam} \bullet 0.5e^{-3})^2}\right) \quad (3)$$

We assume that the cell monolayer cultured on the bottom of the well prevents any contact of the media with the plastic of the well bottom. This assumes 100% cell confluence; in dividing cell-lines this can result in contact inhibition of growth.

2.3. Binding to serum

FBS is routinely included in cell culture medium to supply growth factors, hormones and other factors that support cell growth and improve viability (Gstraunthaler, 2003). Specialist FBS preparations are also available that modify the composition of FBS. For example, charcoal stripped FBS containing no lipid. The major protein in FBS is albumin (> 60% total protein) and this is routinely measured and detailed in the certificate of analysis (CoA) (Zheng et al., 2006). FBS also contains neutral lipids and free fatty acids unless specially treated; the plethora of lipids within FBS is not routinely quantified, but triacylglyceride (TAG) content is reported in the CoA. It is necessary to account for the binding of test compounds to these major serum components in order to determine the true-free concentration in the *in vitro* system. Where the fraction unbound in serum, fu_{FBS} is determined experimentally, it can be used directly in the model. Alternatively, fu_{FBS} can be predicted using Eq. (4).

$$fu_{FBS} = \frac{1}{1 + K_{protein}f_{protein} + \frac{P_{nl}f_{nl,FBS}}{X_{FBS}}} \quad (4)$$

Where $f_{protein}$ (*v*/v) is the fraction of FBS comprised of protein, $K_{protein}$ is the albumin:water partition coefficient, P_{nl} is the neutral lipid partition coefficient (defined below), $f_{nl,FBS}$ is the fraction of FBS comprised of neutral lipid and X_{FBS} is an ionisation term (Table 1), assuming that binding to neutral lipids is limited to unionised species.

Assuming that the fraction of albumin in the FBS is representative of the total protein fraction responsible for protein binding in the FBS, this can be calculated from the mass of albumin reported in the CoA for a batch of FBS using Eq. (5).

$$f_{protein} \approx f_{alb,FBS} = \frac{mass\ albumin \bullet PSV_{albumin}}{1000} \quad (5)$$

Where $PSV_{albumin}$ is the partial specific volume of albumin (0.73 mL/g (Kupke et al., 1972)); it should be noted that Eq. (5) does not in fact yield a true fraction, but the volume of albumin in litres. Here we assume one litre of FBS for the prediction of fu_{FBS}, and so calculation of the volume specific serum components in litres is equivalent to (*v*/v) fractions. The albumin to water partition coefficient, $K_{protein}$, can be determined experimentally or can be calculated as previously described (Endo and Goss, 2011) in Eq. (6); in this work the calculation approach has been used.

Table 1
Calculation of Y and X ionisation terms using Henderson Hasselbalch (Berezhkovskiy, 2011).

Compound Type	Y	X
Neutral	$Y_1 = Y_2 = 0$	$X = 1$
Monoprotic acid	$Y_1 = 10^{pH-pKa}$, $Y_2 = 0$	$X = 1 + Y_1 + Y_2$
Monoprotic base	$Y_1 = 10^{pKa-pH}$, $Y_2 = 0$	$X = 1 + Y_1 + Y_2$
Diprotic acid	$Y_1 = 10^{pH-pKa1} + 10^{pH-pKa2}$, $Y_2 = 10^{2pH-(pKa1+pKa2)}$	$X = 1 + Y_1 + Y_2$
Diprotic base	$Y_1 = 10^{pKa1-pH} + 10^{pKa2-pH}$, $Y_2 = 10^{(pKa1+pKa2)-2pH}$	$X = 1 + Y_1 + Y_2$
Ampholyte	$Y_{1a} = 10^{pH-pKa1}$, $Y_{1b} = 10^{pKa2-pH}$, $Y_2 = 10^{pKa2-pKa1}$	$X = 1 + Y_{1a} + Y_{1b} + Y_2$

Ionisation terms are calculated for the FBS, culture medium, intracellular water, mitochondria and lysosome; for ampholytes, pKa1 corresponds to acidic group and pKa2 to the basic group.

if $logP_{ow} < 4.5$

$$log\,K_{protein} = 1.08 \bullet log\,P_{ow,Tsys} - 0.7$$

if $logP_{ow} \geq 4.5$

$$logK_{protein} = 0.37 \bullet logP_{ow,Tsys} + 2.56 \quad (6)$$

In much the same way, Eq. (7) can be used to calculate a representative (v/v) fraction of neutral lipid in FBS, using TAG as a surrogate for neutral lipid content. TAG concentration is routinely determined using an enzymatic assay and so reported as a molar concentration.

$$f_{nl,FBS} \approx f_{TAG} = \frac{[TAG] \bullet 10^{-3} \bullet MW_{TAG} \bullet PSV_{TAG}}{1000} \quad (7)$$

Where PSV_{TAG} is the partial specific volume of TAG (1.09 mL/g (Deckelbaum et al., 1984)) and the molecular weight of TAG is taken to be 885.453 g/mol; specifically, this corresponds to the molecular weight of trioleate, a TAG molecule comprising a glycerol backbone and three oleic acid residues.

Irrespective of whether fu_{FBS} is determined experimentally or is predicted, its value represents the binding in serum alone. However, serum routinely only comprises a fraction of the complete medium. Consequently, it is necessary to correct the predicted or experimentally determined value to account for the dilution of serum in total culture medium. Firstly, a dilution factor is calculated based on the fraction of serum, f_{serum}, in complete medium Eq. (8) and then an fu_{FBS} value corrected for dilution, $fu_{FBS,dilu}$, calculated Eq. (9).

$$D = \frac{1}{f_{serum}} \quad (8)$$

$$fu_{FBS,dilu} = \frac{fu_{FBS}}{\frac{1}{D} \bullet (1 - fu_{FBS}) + fu_{FBS}} \quad (9)$$

If $f_{serum} = 0$, then $fu_{FBS,dilu} = 1$.

2.4. Partitioning to plastics

In addition to binding to serum components, test compounds may also bind to the plastic of the culture vessel. Here we employ a linear correlation between the plastic to media partition coefficient, $K_{plastic}$, and the octanol to water partition coefficient, P_{OW}, established by (Kramer, 2010) and later used by (Zaldivar Comenges et al., 2017). It

should be noted, that this relationship was established for polycyclic aromatic hydrocarbons (PAHs) and so may not hold true for all classes of compound. In the approach outlined here it is assumed that both unionised and ionised fractions of solubilised compound can bind to culture plastics Eq. (10). It should also be noted that binding to serum components can be considered to be of greater significance than binding to plastics. Indeed, it has been demonstrated that the significance of binding to plastics is reduced with increasing supplementation of FBS in culture media (Kramer et al., 2012).

$$K_{plastic,u} = \frac{C_{plastic}}{C_{medium_{unbound}}} = 10^{0.97 log P_{ow\ Tsys} - 6.94} \tag{10}$$

It is important to note that $k_{plastic}$, unlike other partition coefficients used herein, is not dimensionless and has units of metres (m).

2.5. Partitioning into headspace air

Cells are routinely cultured in humidified incubators to help limit the evaporation of medium. The plate formats utilised in high-throughput assays do not routinely seal individual wells on the plate; lids either cover the entire plate, limiting evaporation, or are handled uncovered due to the use of automated fluidic systems. This means that the volume of air into which compounds solubilised in the media may distribute is poorly defined. The model described here does not take into account the mixing of air above a whole culture plate, or the possible cross-contamination between wells that may occur if multiple volatile compounds or test concentrations are being tested across a single unsealed plate. Here we assume that each well of a plate format exists as an independent, hermetically sealed system.

The exchange of compound between the atmosphere and water is already an established concept in environmental toxicology (Schwarzenbach et al., 2004). At dilute concentrations in pure water, the distribution of neutral compounds between the air and the water is described by the Henry's law constant, K_H Eq. (11).

$$K_H = \frac{P_i}{C_{water_{unbound}}} \tag{11}$$

Where P_i is the partial pressure of the gas phase of the compound (atmLmol^{-1}) and $C_{water\ unbound}$ is the molar concentration in water. Here, it is more convenient to redefine the Henry's law constant of compounds as a dimensionless partition coefficient, $K_{air,u}$ (Eq. (12); also defined as K_{aw}).

$$K = \frac{K_H}{RT} \tag{12}$$

Where R is the universal gas constant and T is the reference temperature in Kelvin (normally 25 °C = 298.15 K). It is important to note that the terms, and therefore the units, in which Henry's law constants are reported are inconsistent and can lead to confusion. In Eq. (12) it is essential that the universal gas constant is expressed in units consistent with those of the Henry's law constant (*i.e.* if K_H is expressed in SI units of Pa m^3 mol^{-1} then R = 8.314 Pa m^3 K^{-1} mol^{-1}; if K_H is expressed in units of atm L mol^{-1} then R = 0.08206 L atm mol^{-1}).

Besides databases listing experimentally determined Henry's law constant values, a number of tools are available for predicting this parameter (Dearden and Schuurmann, 2003; Katritzky et al., 1998). The HenryWin tool gives users a prediction of K_H in SI units, but also as the dimensionless $K_{air} = K_{air,u}$ partition coefficient (Dearden and Schuurmann, 2003).

As already stated above, the Henry's law constant describes the air-water distribution ratio of neutral compounds in non-saturated and pure water, single solute systems. As such, its use here is an approximation of the behaviour in a 'real' aqueous solution containing multiple chemical species. However, to limit the assumptions being made, $K_{air,u}$ is only applied to the unionised fraction, f_{ui}, of solubilised compound.

$$logK_{air,Tsys} = logK_{air} - \frac{\Delta U_{aw}}{ln\,10 \bullet R} \bullet \left(\frac{1}{T_{sys}} - \frac{1}{T_{ref}}\right) \tag{13}$$

Experimental, and predicted values, of Henry's law constant are reported at a reference temperature (T_{ref}) of 25 °C, while the temperature cell culture systems (T_{sys}) is routinely maintained at 37 °C. It is therefore necessary to correct the values used in the model to the relevant system temperature using Eq. (13), where ΔU_{aw} (J mol^{-1}) is the internal energy of phase change for air to water partitioning.

2.6. Partitioning in cells

Using an adapted form of the Rodgers and Rowland approach (Rodgers et al., 2005; Rodgers and Rowland, 2007) we describe the partitioning of test compound into cells. This approach adopts a more mechanistic description of intracellular lipid binding and is based on the pH-partition hypothesis. It assumes that only the unionised fraction can partition across tissue membranes. Therefore, at steady-state, the concentration of unbound, unionised compound between the intracellular and extracellular water is equal Eq. (14).

$$K_{cell\ uu,uu} = \frac{C^{unbound,unionised}_{intracellular}}{C^{unbound,unionised}_{extracellular}} = 1 \tag{14}$$

The unionised concentrations are defined by the Henderson-Hasselbalch equation based on compound type and the local pH (Table 1). In predicting the partitioning of neutral or weak acids/bases, the pH-partition is valid since the compound is unionised or the fraction of ionised compound is negligible and so makes no significant contribution to partitioning across membranes. However, as noted above the negative potential difference maintained across most cell membranes promotes the partitioning of cations into the cell and limits the partitioning of anions.

Using the Fick-Nernst-Planck equation, models for passive cell permeability accounting for differential ionisation (Henderson-Hasselbalch equation), passive permeation of neutral molecules (Fick's law), and passive permeation of ionised molecules (Nernst-Planck equation) across the cell membranes have been published previously (Ghosh et al., 2014a; Ghosh et al., 2014b; Trapp et al., 2008).

Here we adapt the existing Rodgers and Rowland approach incorporating the Fick-Nernst-Planck equation to describe the passive penetration of electrolytes across cell membrane, together with the passive penetration of neutral molecules. $K_{cell\ uu,uu}$ is introduced and derived from the steady-state Fick-Nernst-Planck equation Eqs. (15) and (16), (Table 2) and further used to predict the cell to media partition coefficient (K_{cell}, Eq. (17)).

$$K_{cell\ uu,uu} = \frac{1 + \frac{P^{unbound,ionised\ 1}}{P^{unbound,unionised}} \frac{N_1}{e^{N_1}-1} Y_{1,EW} + \frac{P^{unbound,ionised\ 2}}{P^{unbound,unionised}} \frac{N_2}{e^{N_2}-1} Y_{2,EW}}{1 + \frac{P^{unbound,ionised\ 1}}{P^{unbound,unionised}} \frac{N_1}{e^{N_1}-1} e^{N_1} Y_{IW,1} + \frac{P^{unbound,ionised\ 2}}{P^{unbound,unionised}} \frac{N_2}{e^{N_2}-1} e^{N_2} Y_{IW,2}} \tag{15}$$

Table 2
Nernst-Planck calculations.

Compound type	N
Neutral	$N_1 = 0, N_2 = 0$
Monoprotic acid	$N_1 = -\frac{\varnothing F}{RT}, N_2 = 0$
Monoprotic base	$N_1 = \frac{\varnothing F}{RT}, N_2 = 0$
Diprotic acid	$N_1 = -\frac{\varnothing F}{RT}, N_2 = -\frac{\varnothing F}{RT}$
Diprotic base	$N_1 = \frac{\varnothing F}{RT}, N_2 = \frac{\varnothing F}{RT}$
Ampholyte	$N_{1acid} = -\frac{\varnothing F}{RT}, N_{2base} = \frac{\varnothing F}{RT}, N_2 = \frac{z\varnothing F}{RT}$ (z = 0)

$$K_{IW}{}^{uu,uu}_{organelle} = \frac{1 + \frac{P^{unbound,ionised\ 1}}{P^{unbound,unionised}} \frac{N_1}{e^{N_1}-1} Y_{1,IW} + \frac{P^{unbound,ionised\ 2}}{P^{unbound,unionised}} \frac{N_2}{e^{N2}-1} Y_{2,IW}}{1 + \frac{P^{unbound,ionised\ 1}}{P^{unbound,unionised}} \frac{N_1}{e^{N_1}-1} e^{N_1} Y_{1,organelle} + \frac{P^{unbound,ionised\ 2}}{P^{unbound,unionised}} \frac{N_2}{e^{N_2}-1} e^{N_2} Y_{2,organelle}} \quad (16)$$

Where P is the permeability coefficient of either the ionised or unionised moiety. Using a ratio of the permeability coefficient between the unionised and ionised species we can describe the differential permeability of the two molecular forms. It has previously been assumed that the permeability coefficient of the ionised species is 3–4 log units lower than that of the neutral form (Trapp et al., 2008). Here we assume ionised, unionised permeability coefficient ratios of 2.3 and 3.3 log units for the monoprotic cation and monoprotic anion, respectively; for both diprotic cations and anions we assume a ratio of 10 log units; for ampholytes we assume a ratio of 2 log units.

$$K_{cell,u} = \frac{C_{cell}}{C_{media_{unbound}}} = \begin{pmatrix} (1 - f_{lyso+}f_{mito}) \begin{pmatrix} f_{iw}X_{iw} + P_{nl}f_{nl} + P_{np}f_{np} \\ +K_{aAP}[AP^-](Y_{1,iw} + Y_{2,iw}) \end{pmatrix} \\ + f_{lyso} \begin{pmatrix} f_{iw}X_{lyso} + P_{nl}f_{nl} + P_{np}f_{np} + \\ K_{aAP}[AP^-](Y_{1,lyso} + Y_{2,lyso}) \end{pmatrix} K_{iw\ lyso}^{uu,uu} \\ + f_{mito} \begin{pmatrix} f_{iw}X_{mito} + P_{nl}f_{nl} + P_{np}f_{np} + \\ K_{aAP}[AP^-](Y_{1,mito} + Y_{2,mito}) \end{pmatrix} K_{iw\ mito}^{uu,uu} \end{pmatrix} \frac{1}{X_{ew}} K_{cell\ uu,uu} \quad (17)$$

Eq. (17) is adapted from the original Rodgers and Rowland (Rodgers et al., 2005; Rodgers and Rowland, 2007) approach incorporating $K_{cell\ uu,uu}$ where f_{iw}, f_{lyso}, f_{mito}, f_{nl}, f_{np} denote the fractional cellular volumes of the intracellular water, lysosomes, mitochondria, neutral lipids, and neutral phospholipids, respectively. P_{nl} and P_{np} describe the partitioning of the compound between intracellular water and neutral lipids and neutral phospholipids, respectively. Where the olive oil to water ($P_{vo:w}$) and octanol to water ($P_{o:w}$) partition coefficients are used as surrogates, respectively. $KaAP$ (μM^{-1}) is the acidic phospholipid association constant and [AP^-] is the intracellular acidic phospholipid concentration. This may be determined experimentally for individual compounds or estimated from the blood to plasma ($B:P$) ratio using Eq. (18) (per Rodgers and Rowland (Rodgers et al., 2005; Rodgers and Rowland, 2007)).

$$K_{aAP} = \left[\frac{\frac{haem - 1 + B:P}{haem}}{fu} \bullet \frac{X_{plasma}}{K_{RBC\ uu,uu}} - (f_{iwRBC} \bullet X_{IW,RBC} + P_{nl} \bullet f_{nl,RBC} + P_{np} \bullet f_{np,RBC}) \right] \bullet \frac{1}{[AP^-]_{RBC} \bullet (Y_{1,RBC} + Y_{2,RBC})} \quad (18)$$

As with Henry's law constant, experimentally determined $P_{o:w}$ values, and predicted values, are reported at a reference temperature of 25 °C and these too must be corrected to correspond to the relevant system temperature before being used in as model inputs, Eq. (19); where ΔU_{ow} (J mol^{-1}) is the internal energy of phase change for octanol to water partitioning.

$$logP_{ow,Tsys} = logP_{ow} - \frac{\Delta U_{ow}}{ln\,10 \bullet R} \bullet \left(\frac{1}{T_{sys}} - \frac{1}{T_{ref}} \right) \quad (19)$$

As well as the incorporation of $K_{cell\ uu,uu}$, Eq. (17) has two further modifications beyond the original Rodgers and Rowland approach. Firstly, there is no longer a need to incorporate the fraction of extracellular water in tissues or binding to extracellular proteins present in the extracellular water since this fraction will be absent in 2D cell culture systems. Secondly, the equation is adapted so that two subcellular organelle compartments (lysosome and mitochondria) are considered.

While Eq. (17) allows the calculation of total intracellular concentrations, it is necessary to determine separate cellular compartment to medium ratios to be able to calculate the concentration within respective cellular compartment; for details see the *supplementary material.*

2.7. Apparent in vitro volume of distribution at steady-state

Using the partitioning coefficients, serum-binding and system parameters described above, we can predict the apparent *in vitro* volume of distribution at steady-state, Eq. (20), thus generating a prediction of the unbound, freely dissolved media concentration.

$$C_{medium,dissolved,u} = \frac{C_{nominal} \bullet fu_{FBS,dilu} \bullet V_{medium}}{V_{medium} + K_{air}f_{ui}V_{air} + K_{cell}V_{totalcell} + K_{plastic}SA_{media} \bullet 10^3} \quad (20)$$

Subsequently, the steady-state concentration in each compartment of the model can be predicted based on the respective partition coefficient and the unbound, freely dissolved media concentration Eqs. (21), (22) and (23).

$$C_{air} = K_{air,u} \bullet f_{ui} \bullet C_{medium,dissolved,u}$$

$$if\ V_{air} = 0,\ C_{air} = 0 \quad (21)$$

$$C_{plastic} = K_{plastic,u} \bullet C_{medium,dissolved,u} \bullet 10^3 \quad (22)$$

$$C_{cell} = K_{cell,u} \bullet C_{medium,dissolved,u} \quad (23)$$

2.8. Quasi steady-state dynamic modelling

The partition model presented defines the system at steady-state. To test the potential impact of the steady-state assumption, we formulated a dynamic variant of the model incorporating the instantaneous rate of metabolism or loss from the system by the following differential equation, Eq. (24).

$$\frac{dQ_{met}(t)}{dt} = n_{cell} \bullet CL_{int,met} \bullet C_{cell}(t) \quad (24)$$

Where $Q_{met}(t)$ is the quantity metabolized in moles up to time t, $CL_{int,met}$ (L min^{-1}) is the intrinsic metabolic clearance per cell, and n_{cell} is the number of cells in the cultured monolayer. The total quantity of parent chemical remaining in the system at time t, $Q_{total}(t)$, can then be calculated, Eq. (25).

$$Q_{total}(t) = C_{nominal} \bullet V_{media} - Q_{met}(t) \quad (25)$$

In Eq. (24), $C_{cell}(t)$ is computed using Eqs. (20) and (23), replacing $C_{nominal}$ by $\frac{Q_{total}(t)}{V_{media}}$ at each integration time step; Eqs. (21) to (23) apply without change. This quasi-steady-state differential formulation is flexible and could be easily modified to describe nonlinear metabolism or other *in vitro* elimination processes if needed. In its current linear form, its analytical solution is known and could be used. However, for the simulation results presented in the following we numerically integrated the differential equation above.

2.9. Code and simulations

The static model equations have been coded in R (R Core Team, 2018), and GNU MCSim (Bois, 2009) for the dynamic model.

3. Results

3.1. Steady-state model

We performed representative simulations of the steady-state distribution of 1194 compounds with diverse physicochemical properties

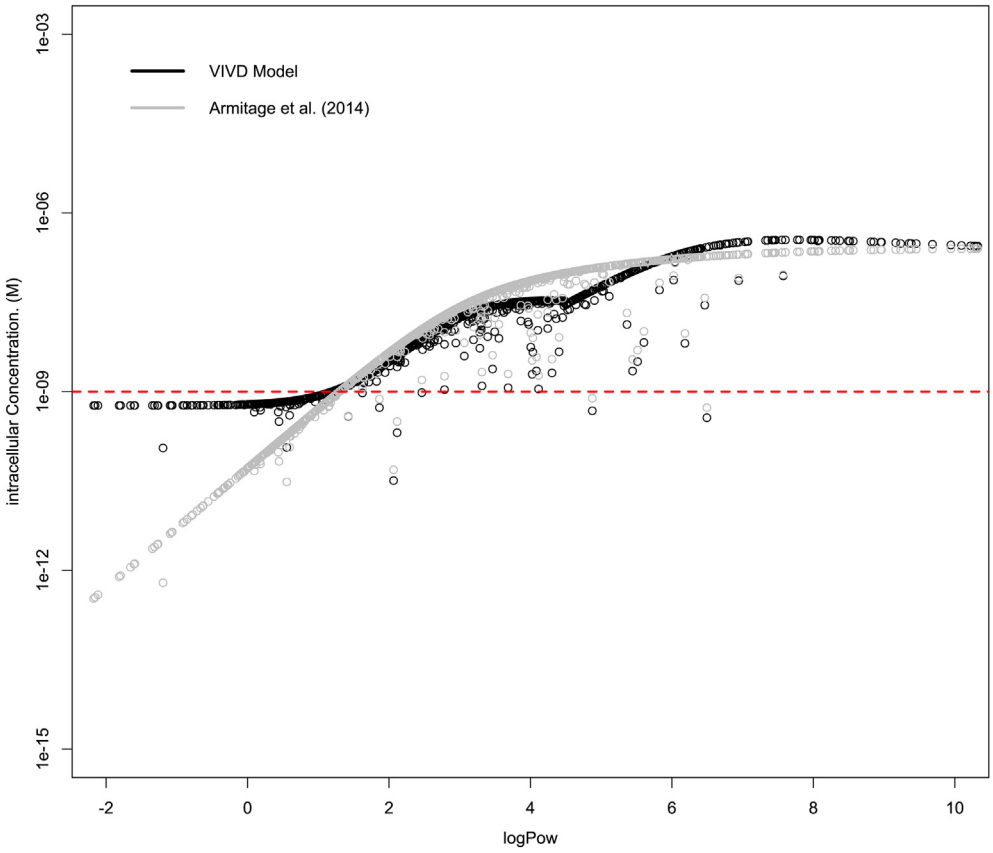

Fig. 1. Comparative simulations of steady-state distribution *in vitro* with the previously published (9) (grey) and VIVD model (black) assuming neutrality; simulations represent primary human hepatocytes cultured in 10% FBS containing 24 and 1.9 gL^{-1} of albumin and TAG, respectively treated with 1 nM (red dotted line) of each test compound individually.

in an adherent monolayer of primary human hepatocytes cultured in 10% FBS assuming a 1 nM nominal treatment concentration similar to Armitage and colleagues (Armitage et al., 2014). Firstly, steady-state distribution was simulated assuming no significant ionisation of test compounds; under this assumption the VIVD model shows largely comparable predictions of total intracellular concentration to that previously published (Armitage et al., 2014) (Fig. 1).

This is to be expected given the underlying assumptions of the respective models; here we describe the distribution into cells based on the partitioning into the intracellular water as well as the binding to cellular neutral lipids and phospholipids. Although our model does account for binding to cellular acidic phospholipids, as we assume that this is only relevant for significantly ionised basic compounds and so does not contribute to the intracellular binding of neutral compounds. The Armitage model (Armitage et al., 2014) defines partitioning into cells based on the fraction of the cell comprised of lipids, f_{lipid}, and the octanol to water partition coefficient Eq. (26).

$$K_{cell} = f_{lipid} P_{ow} \tag{26}$$

The total fraction of the cell comprised of neutral lipids and phospholipids in our model is very similar to that in simulations with the Armitage model (0.06 *versus* 0.05, respectively) and so for neutral compounds we would expect comparable predictions. However, like the model recently published by Fischer *et al* (Fischer et al., 2017), our VIVD model also incorporates the partitioning of test compound between the medium water and intracellular water and so predicts higher intracellular concentrations at $\log P_{ow} < 1$.

Simulating the same cell culture system, but incorporating simulated, randomly assigned, differential ionisation of test compounds, rather than the assumption of neutrality, we see significant differences in the predicted total intracellular concentrations (Fig. 2). Moderate to strong bases (pKa ≥ 7) show significantly higher partitioning into cells than would be predicted assuming neutrality. In part this is attributable to the differential ionisation of basic compounds between the culture medium (pH = 7.4) and the intracellular water (pH = 7.0). The fraction ionised in the intracellular water exceeds that in the culture medium, with this fraction having reduced membrane permeability, relative to the neutral fraction, resulting in an increased proportion of the free dose entering and remaining within the cells. Additionally, while the ionised fraction of compound within the culture media has reduced membrane permeability, the negative membrane across the hepatocyte cell membrane (Φ = -70 mV) increases the apparent permeability of ionised (cationic) bases. Conversely, significantly ionised acids show reduced predicted partitioning into cells when ion permeability and the impact of membrane potential are considered within the model, due to ionisation in the culture media and the limiting effect of the negative membrane potential on the ionised (anionic) fraction. The total intracellular concentrations predicted under the two different model assumptions can differ by many orders of magnitude and so could significantly impact the *in vitro* to *in vivo* extrapolation of toxicity endpoints quantified *in vitro*.

The prediction of binding to components within serum is predominantly driven by $\log P_{o:w}$ even with accounting for ionisation within the model framework. Binding to serum albumin is the most significant contributor to fu_{FBS} and, since the model assumes that ionisation does not impact a compound's ability to bind to albumin, the assumption that only the unionised fraction of test compound binds to serum triglycerides has a minimal effect on overall serum binding in our simulations (Fig. 3). Although the prediction of fu_{FBS} accounts for ionisation, it does not differentiate between ionised species (*i.e.* acids *vs* bases).

3.2. Quasi steady-state dynamic dynamic model

For 612 of the 1194 chemicals considered (Armitage et al., 2014), we have used hepatic metabolic clearance estimates reported in the *R*

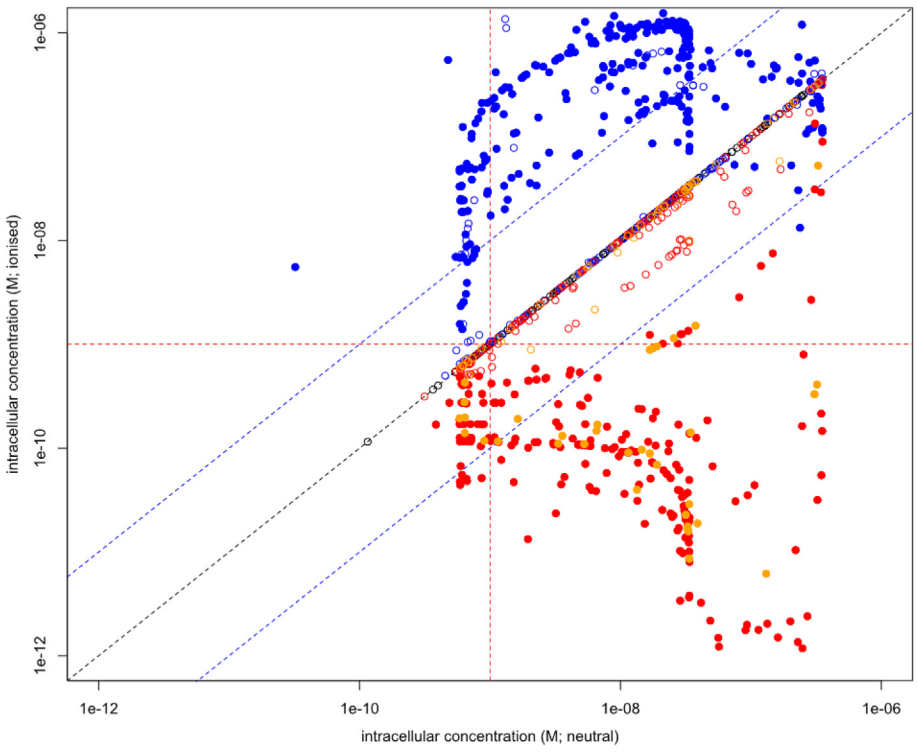

Fig. 2. Comparative simulations of steady-state distribution *in vitro* with the VIVD model assuming neutrality (x-axis) and accounting for ionisation (y-axis); simulations represent primary human hepatocytes cultured in 10% FBS containing 24 and 1.9 gL^{-1} of albumin and TAG, respectively treated with 1 nM (red dotted line) of each test compound individually; acids (red), bases (blue), ampholytes (orange). The black dotted line represents unity, blue dotted lines represent 10-fold, compounds with fraction unionised < 0.1 (pH = 7) plotted as solid data points.

package *httk* (Wambaugh et al., 2018) (v1.7). Those estimates were corrected for the fraction unbound in medium by Wambaugh (Wambaugh et al., 2018) and colleagues, but not for the partitioning into cells (*i.e.* for the partition coefficient $K_{cell,u}$) so we divided the values given in *httk* by that parameter, correcting units as required. For those 612 chemicals, using our dynamic model, we performed simulations of the time courses over 48 h for the quantity of parent chemical remaining in the system and for the intracellular cellular concentration, following a single treatment at a nominal concentration of 1 nM, Fig. 4. For the majority of the 612 chemicals, metabolism has an impact; 283 have been > 90% metabolized and 165 of them have been between 10 and 90% metabolized. Under the quasi-steady-state assumptions, the concentrations in cells, and other *in vitro* compartments are affected to the same proportion. This demonstrates that the steady-state model would over-predict intracellular exposure in metabolically competent *in vitro* cell systems for the majority of the 612 subset of compounds.

4. Discussion

Here we present a pragmatic modelling approach for predicting the distribution of test compounds in *in vitro* cell culture systems. The aim is to predict the intracellular concentration accounting for binding to serum components, culture plastics, and accounting for distribution into the air in the headspace above the culture medium, and binding to cellular lipids. The approach detailed above expands on previously published approaches (Armitage et al., 2014; Fischer et al., 2017; Zaldivar Comenges et al., 2017) by incorporating differential ionisation of test compounds between the intracellular water and the aqueous culture media, ion-permeability across cell membranes, and the effect of membrane potential. Our results show that predicted intracellular concentrations differ considerably dependent on whether the model used disregards the impact of compound ionisation (*i.e.* all compounds are neutral) or accounts for compound ionisation. While the

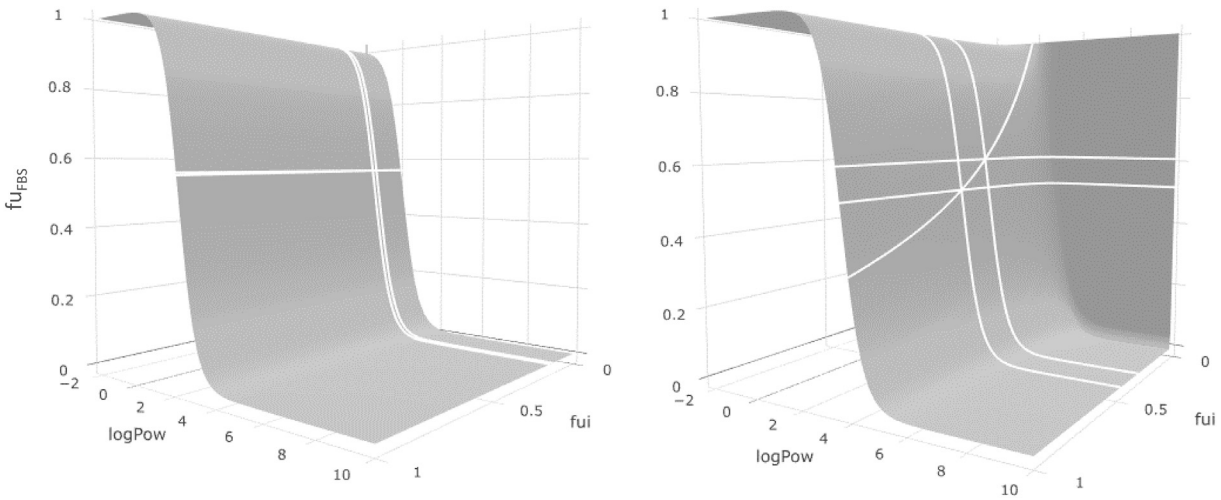

Fig. 3. Predicted fraction unbound in fetal bovine; serum containing 24 and 1.9 gL^{-1} of albumin and TAG, respectively (left), serum containing 0 and 1.9 gL^{-1} of albumin and TAG, respectively (right).

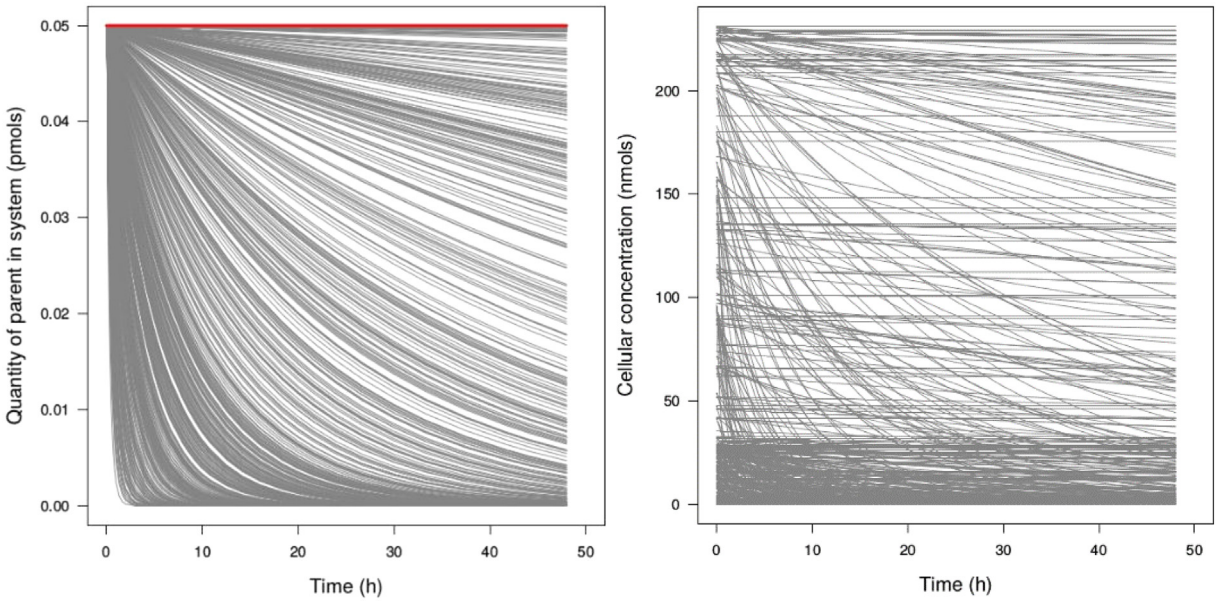

Fig. 4. Predictions of the quantity-time profile of parent chemical in the assay system (left) and of its intracellular concentration-time profile (right); predictions assuming no metabolism (red line) and incorporating metabolism (grey lines) for 612 chemicals.

partitioning of compound between culture medium and cells in our model is based upon the previously published work of Rodgers and Rowland (Rodgers et al., 2005; Rodgers and Rowland, 2007), we revise a fundamental assumption incorporating the permeability of the ionised species, rather than assuming that only the unionised form will partition across the membrane.

With the exception of toxicities mediated through targets presented at the cell surface, the unbound intracellular concentration is the most directly relevant operating concentration driving toxicological endpoints observed *in vitro*, and therefore the most translatable to *in vivo* scenarios. Previous publications have sought to improve on the IVIVE of concentration-dependent toxicity by correcting for binding to serum-supplemented culture medium, so translating the unbound effect concentration *in vitro* to the unbound plasma concentration *in vivo* (Gulden and Seibert, 2003). External *in vivo* doses required to achieve the unbound effect-concentration, determined *in vitro* can then be predicted based upon reverse-dosimetry using physiologically-based pharmacokinetic (PBPK) models. However, while representative at many levels of their tissue of origin, isolated primary cells or immortalised/transformed cell lines are very different to *in vivo* tissues lacking key structural elements (*e.g.* interstitial fluid). As such, the most translatable operating concentration from *in vitro* is the intracellular concentration, which can inform a reverse-dosimetry approach using PBPK models describing the distribution of compounds into tissues, incorporating extracellular water and tissue blood flow.

A balance must be struck between the pragmatic approach presented here, and more complex models (Zaldivar Comenges et al., 2017). The model presented here predicts *in vitro* distribution at steady-state; while this is an acceptable approximation for predictions in non-proliferating cell systems with low metabolic capacity or stable compounds, it could be misleading if these model assumptions are in conflict with the reality of the cell culture system being used. This would be important for example if trying to predict intracellular concentrations in 3D culture systems, hanging droplet or spheroid systems, or organ on a chip/micro-physiological systems. We demonstrate the impact of metabolic clearance on predictions relative to the steady-state model with a quasi-steady-state dynamic version of the model that is applicable in metabolically competent cellular systems, such as primary human hepatocytes. The subset of 612 chemicals used for the dynamic system simulations cannot be taken as a representative sample of all chemicals. However, it demonstrates that in a metabolically competent assay system, metabolism can have a large impact on intracellular exposure. In that case, the dynamic version of the model should be used to obtain more accurate estimates of effective dose. As noted above, the quasi-steady-state differential formulation is flexible and could describe other *in vitro* elimination processes if needed. Such an adaption should be considered when simulating the distribution of highly volatile compounds in *in vitro* assays. In a non-hermetically sealed system, the loss of compound to the air represents a clearance mechanism that would lead to over-prediction of intracellular concentrations by the model under steady-state assumptions. Outputs from the steady-state model showing significant distribution of test compound into the headspace, will identify the need for users to consider whether the model assumptions are fit for purpose or necessitate revision. It may also identify the need for further considerations in laboratory safety when performing assays, and so may inform protocol design.

5. Conclusion

In vitro toxicity assays are increasingly being used to identify chemical hazards to human and animal health and inform risk assessment. Consequently, these systems must be well characterised and the kinetics understood in order to extract the correct parameters and better interpret the toxicity markers monitored *in vitro*. Ultimately, such an approach will better inform quantitative *in vitro* to *in vivo* extrapolation and elucidate mechanistic insight as part of a systems toxicology approach (Hartung et al., 2017). While only limited verification of such models has been published to date, and further experimental work are warranted (Bellwon et al., 2015; Kramer et al., 2012), model development and verification will need to be performed in tandem to the development of increasingly sophisticated *in vitro* systems in order to assess the impact of *in vitro* distribution and facilitate the robust IVIVE of chemical hazard (Pamies and Hartung, 2017).

Competing interests

Fisher, Gardner, and Jamei are all employees of Certara UK Limited (Simcyp Division). Siméon and Bois are both employees of INERIES, METO Unit.

Acknowledgement

This project has received funding from the European Union's Horizon 2020 research and innovation programme under grant agreement No 681002.

References

Armitage, J.M., Wania, F., Arnot, J.A., 2014. Application of mass balance models and the chemical activity concept to facilitate the use of in vitro toxicity data for risk assessment. Environ. Sci. Technol. 48, 9770–9779.

Bell, S.M., Chang, X., Wambaugh, J.F., Allen, D.G., Bartels, M., Brouwer, K.L.R., Casey, W.M., Choksi, N., Ferguson, S.S., Fraczkiewicz, G., Jarabek, A.M., Ke, A., Lumen, A., Lynn, S.G., Paini, A., Price, P.S., Ring, C., Simon, T.W., Sipes, N.S., Sprankle, C.S., Strickland, J., Troutman, J., Wetmore, B.A., Kleinstreuer, N.C., 2018. In vitro to in vivo extrapolation for high throughput prioritization and decision making. Toxicol. In Vitro 47, 213–227.

Bellwon, P., Truisi, G.L., Bois, F.Y., Wilmes, A., Schmidt, T., Savary, C.C., Parmentier, C., Hewitt, P.G., Schmal, O., Josse, R., Richert, L., Guillouzo, A., Mueller, S.O., Jennings, P., Testai, E., Dekant, W., 2015. Kinetics and dynamics of cyclosporine a in three hepatic cell culture systems. Toxicol. In Vitro 30, 62–78.

Berezhkovskiy, L.M., 2011. The corrected traditional equations for calculation of hepatic clearance that account for the difference in drug ionization in extracellular and intracellular tissue water and the corresponding corrected PBPK equation. J. Pharm. Sci. 100, 1167–1183.

Blaauboer, B.J., 2010. Biokinetic modeling and in vitro-in vivo extrapolations. J. Toxicol. Environ. Health B Crit. Rev. 13, 242–252.

Bois, F.Y., 2009. GNU MCSim: Bayesian statistical inference for SBML-coded systems biology models. Bioinformatics 25, 1453–1454.

Core Team, R., 2018. R: A Language and Environment for Statistical Computing. R Foundation for Statistical Computing, Vienna, Austria.

Dearden, J.C., Schuurmann, G., 2003. Quantitative structure-property relationships for predicting Henry's law constant from molecular structure. Environ. Toxicol. Chem. 22, 1755–1770.

Deckelbaum, R.J., Granot, E., Oschry, Y., Rose, L., Eisenberg, S., 1984. Plasma triglyceride determines structure-composition in low and high density lipoproteins. Arteriosclerosis 4, 225–231.

Endo, S., Goss, K.U., 2011. Serum albumin binding of structurally diverse neutral organic compounds: data and models. Chem. Res. Toxicol. 24, 2293–2301.

Fischer, F.C., Henneberger, L., Konig, M., Bittermann, K., Linden, L., Goss, K.U., Escher, B.I., 2017. Modeling exposure in the Tox21 in vitro Bioassays. Chem. Res. Toxicol. 30, 1197–1208.

Ghosh, A., Maurer, T.S., Litchfield, J.E., Varma, M.V., Rotter, C.J., Scialis, R., Feng, B., Tu, M., Guimaraes, C.R.W., Scott, D.O., 2014a. Towards a unified model of passive drug permeation II: the physiochemical determinants of unbound tissue distribution with applications to the design of hepatoselective glucokinase activators. Drug Metab. Dispos. 42, 1599–1610.

Ghosh, A., Scott, D.O., Maurer, T.S., 2014b. Towards a unified model of passive drug permeation I: origins of the unstirred water layer with applications to ionic permeation. Eur. J. Pharm. Sci. 52, 109–124.

Gibb, S., 2008. Toxicity testing in the 21st century: a vision and a strategy. Reprod. Toxicol. 25, 136–138.

Godoy, P., Hewitt, N.J., Albrecht, U., Andersen, M.E., Ansari, N., Bhattacharya, S., Bode, J.G., Bolleyn, J., Borner, C., Bottger, J., Braeuning, A., Budinsky, R.A., Burkhardt, B., Cameron, N.R., Camussi, G., Cho, C.S., Choi, Y.J., Craig Rowlands, J., Dahmen, U., Damm, G., Dirsch, O., Donato, M.T., Dong, J., Dooley, S., Drasdo, D., Eakins, R., Ferreira, K.S., Fonsato, V., Fraczek, J., Gebhardt, R., Gibson, A., Glanemann, M., Goldring, C.E., Gomez-Lechon, M.J., Groothuis, G.M., Gustavsson, L., Guyot, C., Hallifax, D., Hammad, S., Hayward, A., Haussinger, D., Hellerbrand, C., Hewitt, P., Hoehme, S., Holzhutter, H.G., Houston, J.B., Hrach, J., Ito, K., Jaeschke, H., Keitel, V., Kelm, J.M., Kevin Park, B., Kordes, C., Kullak-Ublick, G.A., LeCluyse, E.L., Lu, P., Luebke-Wheeler, J., Lutz, A., Maltman, D.J., Matz-Soja, M., McMullen, P., Merfort, I., Messner, S., Meyer, C., Mwinyi, J., Naisbitt, D.J., Nussler, A.K., Olinga, P., Pampaloni, F., Pi, J., Pluta, L., Przyborski, S.A., Ramachandran, A., Rogiers, V., Rowe, C., Schelcher, C., Schmich, K., Schwarz, M., Singh, B., Stelzer, E.H., Stieger, B., Stober, R., Sugiyama, Y., Tetta, C., Thasler, W.E., Vanhaecke, T., Vinken, M., Weiss, T.S., Widera, A., Woods, C.G., Xu, J.J., Yarborough, K.M., Hengstler, J.G., 2013. Recent advances in 2D and 3D in vitro systems using primary hepatocytes, alternative hepatocyte sources and non-parenchymal liver cells and their use in investigating mechanisms of hepatotoxicity, cell signaling and ADME. Arch. Toxicol. 87, 1315–1530.

Gstraunthaler, G., 2003. Alternatives to the use of fetal bovine serum: serum-free cell culture. ALTEX 20, 275–281.

Gulden, M., Seibert, H., 2003. In vitro-in vivo extrapolation: estimation of human serum concentrations of chemicals equivalent to cytotoxic concentrations in vitro. Toxicology 189, 211–222.

Hartung, T., FitzGerald, R.E., Jennings, P., Mirams, G.R., Peitsch, M.C., Rostami-Hodjegan, A., Shah, I., Wilks, M.F., Sturla, S.J., 2017. Systems toxicology: real world applications and opportunities. Chem. Res. Toxicol. 30, 870–882.

Hoehme, S., Brulport, M., Bauer, A., Bedawy, E., Schormann, W., Hermes, M., Puppe, V., Gebhardt, R., Zellmer, S., Schwarz, M., Bockamp, E., Timmel, T., Hengstler, J.G., Drasdo, D., 2010. Prediction and validation of cell alignment along microvessels as order principle to restore tissue architecture in liver regeneration. Proc. Natl. Acad. Sci. U. S. A. 107, 10371–10376.

Holmes, A.M., Creton, S., Chapman, K., 2010. Working in partnership to advance the 3Rs in toxicity testing. Toxicology 267, 14–19.

Katritzky, A.R., Wang, Y., Sild, S., Tamm, T., 1998. QSPR studies on vapor pressure, aqueous solubility, and the prediction of water-air partition coefficients. J. Chem. Inf. Comput. Sci. 38, 720–725.

Kazmi, F., Hensley, T., Pope, C., Funk, R.S., Loewen, G.J., Buckley, D.B., Parkinson, A., 2013. Lysosomal sequestration (trapping) of lipophilic amine (cationic amphiphilic) drugs in immortalized human hepatocytes (Fa2N-4 cells). Drug Metab. Dispos. 41, 897–905.

Kramer, N.I., 2010. Measuring, Modelling and Increasing the Free Concentration of Test Chemicals in Cell Assays (PhD Thesis). Utrecht University, Utrecht, Netherlands.

Kramer, N.I., Krismartina, M., Rico-Rico, A., Blaauboer, B.J., Hermens, J.L., 2012. Quantifying processes determining the free concentration of phenanthrene in Basal cytotoxicity assays. Chem. Res. Toxicol. 25, 436–445.

Kupke, D.W., Hodgins, M.G., Beams, J.W., 1972. Simultaneous determination of viscosity and density of protein solutions by magnetic suspension. Proc. Natl. Acad. Sci. U. S. A. 69, 2258–2262.

Leist, M., Ghallab, A., Graepel, R., Marchan, R., Hassan, R., Bennekou, S.H., Limonciel, A., Vinken, M., Schildknecht, S., Waldmann, T., Danen, E., van Ravenzwaay, B., Kamp, H., Gardner, I., Godoy, P., Bois, F.Y., Braeuning, A., Reif, R., Oesch, F., Drasdo, D., Hohme, S., Schwarz, M., Hartung, T., Braunbeck, T., Beltman, J., Vrieling, H., Sanz, F., Forsby, A., Gadaleta, D., Fisher, C., Kelm, J., Fluri, D., Ecker, G., Zdrazil, B., Terron, A., Jennings, P., van der Burg, B., Dooley, S., Meijer, A.H., Willighagen, E., Martens, M., Evelo, C., Mombelli, E., Taboureau, O., Mantovani, A., Hardy, B., Koch, B., Escher, S., van Thriel, C., Cadenas, C., Kroese, D., van de Water, B., Hengstler, J.G., 2017. Adverse outcome pathways: opportunities, limitations and open questions. Arch. Toxicol. 91, 3477–3505.

Meek, M.E., Lipscomb, J.C., 2015. Gaining acceptance for the use of in vitro toxicity assays and QIVIVE in regulatory risk assessment. Toxicology 332, 112–123.

Pamies, D., Hartung, T., 2017. 21st century cell culture for 21st century toxicology. Chem. Res. Toxicol. 30, 43–52.

Rodgers, T., Rowland, M., 2007. Physiologically-based pharmacokinetic modeling 2: predicting the tissue distribution of acids, very weak bases, neutrals and zwitterions. J. Pharm. Sci. 95, 1238–1257.

Rodgers, T., Leahy, D., Rowland, M., 2005. Physiologically based pharmacokinetic modeling 1: predicting the tissue distribution of moderate-to-strong bases. J. Pharm. Sci. 94, 1259–1276.

Schwarzenbach, R.P., Gschwen, P.M., Imoden, D.M., 2004. Environmental Organic Chemistry. J. Wiley and Sons.

Schwen, L.O., Schenk, A., Kreutz, C., Timmer, J., Bartolome Rodriguez, M.M., Kuepfer, L., Preusser, T., 2015. Representative sinusoids for hepatic four-scale pharmacokinetics simulations. PLoS One 10, e0133653.

Tice, R.R., Austin, C.P., Kavlock, R.J., Bucher, J.R., 2013. Improving the human hazard characterization of chemicals: a Tox21 update. Environ. Health Perspect. 121, 756–765.

Trapp, S., Rosania, G.R., Horobin, R.W., Kornhuber, J., 2008. Quantitative modeling of selective lysosomal targeting for drug design. Eur. Biophys. J. 37, 1317–1328.

Wambaugh, J.F., Hughes, M.F., Ring, C.L., MacMillan, D.K., Ford, J., Fennell, T.R., Black, S.R., Snyder, R.W., Sipes, N.S., Wetmore, B.A., Westerhout, J., Setzer, R.W., Pearce, R.G., Simmons, J.E., Thomas, R.S., 2018. Evaluating in vitro-in vivo extrapolation of toxicokinetics. Toxicol. Sci. 163, 152–169.

Worth, A.P., Louisse, J., Macko, P., Sala Benito, J.V., Paini, A., 2017. Virtual cell based assay simulations of intra-mitochondrial concentrations in hepatocytes and cardiomyocytes. Toxicol. In Vitro 45, 222–232.

Zaldivar Comenges, J.M., Joossens, E., Benito, J.V.S., Worth, A., Paini, A., 2017. Theoretical and mathematical foundation of the virtual cell based assay - a review. Toxicol. In Vitro 45, 209–221.

Zheng, X., Baker, H., Hancock, W.S., Fawaz, F., McCaman, M., Pungor Jr., E., 2006. Proteomic analysis for the assessment of different lots of fetal bovine serum as a raw material for cell culture. Part IV. application of proteomics to the manufacture of biological drugs. Biotechnol. Prog. 22, 1294–1300.